OPTIMIZING ULTRASONIC WELDING PARAMETERS FOR CARBON FIBER REINFORCED THERMOPLASTIC COMPOSITE PLIES

Harry K. Lee
School of Mechanical Engineering, Purdue University
Composite Manufacturing and Simulation Center (CMSC), Purdue University
West Lafayette, Indiana/United States of America 47906
Garam Kim
School of Aviation and Transportation Technology, Purdue University
Composite Manufacturing and Simulation Center (CMSC), Purdue University
West Lafayette, Indiana/United States of America 47906
Eduardo V. Barocio
Composite Manufacturing and Simulation Center (CMSC), Purdue University
West Lafayette, Indiana/United States of America 47906

Abstract

Ultrasonic spot welding is often used to fix continuous fiber-reinforced thermoplastic composite plies before consolidation. However, the temperature development during the ultrasonic spot welding of multiple fiber reinforced thermoplastic composite plies is not yet fully understood, and there are no guidelines for choosing an optimal welding parameter. Improper ultrasonic welding parameters can cause thermal degradation, fiber breakage, warping, or incomplete welds. In this research, welding amplitudes ranging from 15 to 75 µm were tested by welding 8 plies of continuous carbon fiber-reinforced polyether ketone ketone (PEKK) composite plies. A thermal camera was used to measure the temperature development and distribution over time during the welding process. The transient thermal response revealed three stages during a successful welding process using 45 µm amplitude, which have been identified as build-up, welding, and steady-state stage. Lower amplitudes resulted in incomplete welds, and higher amplitudes showed an overshoot in the temperature. While higher amplitudes result in faster weld time, the unnecessary overshoot in temperature can cause thermal degradation to the polymer matrix and cause undesired fiber distortions.

Keywords: Thermoplastic composites, ultrasonic welding, thermoforming

Introduction

Fiber-reinforced composites have various advantages over other materials for industries such as the aerospace and automotive industries. Fiber-reinforced composites are known as advanced composites for their exceptional material properties. Compared to traditional metals, the continuous fiber-reinforced composites have a high strength to weight ratio, stiffness, corrosion resistance, fatigue resistance, and design flexibility [1,2]. Recently, thermoplastic composites are receiving attention due to their advantages, such as high impact and abrasion resistance [2,3]. In the context of manufacturing, the production time is typically lower for thermoplastic, as it takes longer to run cure cycles for thermoset polymers. The shelf life of thermoplastic is significantly longer compared to thermoset as thermoset polymers gradually cure even at freezing temperatures. Manufacturing processes of thermoplastic composite parts also have lower environmental impact as they do not produce volatile organic compounds like the chemical reactions from thermoset polymers. Thermoplastic composite parts are often recyclable while recycling thermoset composites is challenging since it is not reformable once cured [1–3].

Thermoforming is a thermoplastic manufacturing process for thin-walled geometries utilizing heat and pressure [1–6]. It has been adopted by the thermoplastic composite industry for its low cycle time and cost efficiency. While the thermoforming process can be applied to any pre-consolidated laminate, this study focuses on laminates made from continuous fiber-reinforced thermoplastic prepreg. In this context, the entire manufacturing process can be separated into three major steps which are lay-up, consolidation, and thermoforming. This is illustrated in Figure 1. Thermoforming of continuous fiber-reinforced thermoplastic composites starts with laying up layers of prepreg and consolidating them into a single laminate. Then during thermoforming, the pre-consolidated laminate is reheated, often with an infrared (I/R) heater and stamped using a heated platen press with male and female tools. This process is performed above the glass transition temperature for amorphous thermoplastics and above the melting temperature for semi-crystalline thermoplastics [1–3].

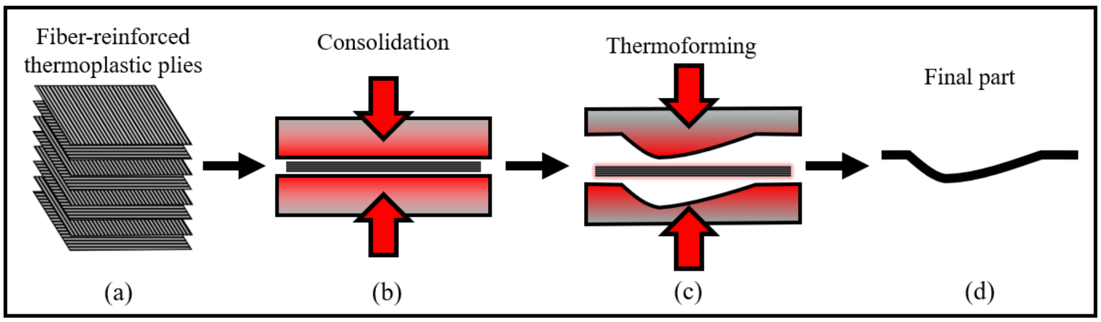

Figure 1. Major steps of pre-consolidation and thermoforming of a continuous fiber-reinforced thermoplastic composite part

While it seems repetitive, experimental studies have shown that pre-consolidation into a flat laminate minimizes voids, and consequentially improves the part quality such as porosity level, crystallinity, and interlaminar bond strength [1,4–7]. However, thermoforming a pre-consolidated 2D laminate into a 3D part comes with many challenges such as wrinkling and buckling, illustrated in Figure 2. Traditional 2D blanks also cannot create parts with variable thickness without creating a polymer rich area, because a pre-consolidated blank has a uniform number of plies throughout itself.

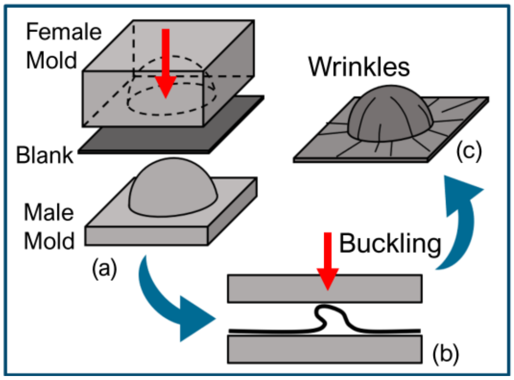

Figure 2. Example of buckling and wrinkling during thermoforming of dome shaped geometry using traditional 2-dimensional blanks

Alternative to pre-consolidated 2D blanks, innovations in automated fiber placement (AFP) and automated tape placement (ATP) have shown potential for partially consolidated tailored blanks. Tailored blanks are different from traditional 2D blanks in that their partially consolidated geometry is very close to the final part geometry. This prevents wrinkling and buckling as well as reduce material waste. Tailored blanks also allow for fiber discontinuity as specified locations (darts), to allow for more aggressive reshaping during the thermoforming process, shown in Figure 3. Partial consolidation or locally bonding of the plies also allow easier inter-ply slipping allowing more complex final part geometry. Lastly, the potential for varying sizes and shapes of tailored blanks allows varying number of plies, and thus allows varying thickness in the final part geometry. The exclusion of complete pre-consolidation may result in sacrificing final part quality, but the benefits of tailored partially consolidated blanks outweigh the loss. Many ATP processes utilize ultrasonic spat welding (USSW) to partially consolidate or locally bond the plies together. The rapid development in ATP and AFP have also been successfully working to minimize any voids and other part quality issues.

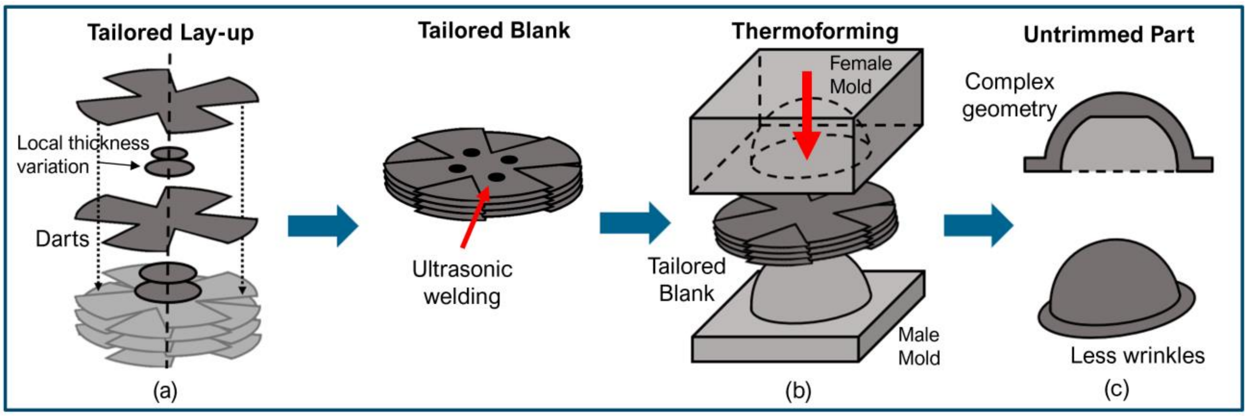

Figure 3. Thermoforming of a dome shaped geometry using a tailored blank

Ultrasonic welding is a type of fusion bonding with which the material at the bonding interface is locally heated, diffused, and then cooled. Ultrasonic welding achieves this by applying vertical mechanical vibrations to cause molecular friction and generate thermal energy. Ultrasonic welding [8,9] is used in plastic and metal assemblies for joining parts together and is noted for the short processing time and cost efficiency compared to the use of mechanical fastenings and adhesive bonding. An ultrasonic welder consists of a generator, a converter or transducer, a booster, a sonotrode (horn), and an anvil as illustrated in Figure 4. The generator creates an electrical signal at high frequency (20-40 kHz). The converter then transforms the electrical signals into mechanical vibrations with amplitude typically around 10-20 µm. The booster amplifies the mechanical vibrations transferred to the welding horn by a constant gain. The main purpose of the horn is to transfer mechanical energy into the sample. The geometry of the horn can affect the amplify the mechanical vibrations, resulting in a constant gain. The resulting amplitude can range around 10-120 µm or more depending on the application. The anvil secures the samples for adequate delivery of mechanical energy.

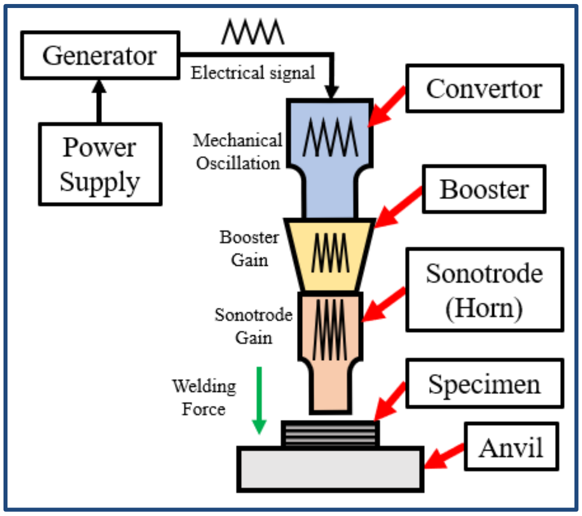

Figure 4. Schematic of an ultrasonic welding system and its major components

There are many welding processing parameters that can be controlled during ultrasonic welding [8,9]. The amplitude is the peak-to-peak travel distance of the tip of the horn. The duration of the welding process is controlled by the generator and often depends on weld time or amount of energy delivered. As the energy is transferred by mechanical vibrations, the welding force is another important parameter. The welding force is the force applied on the horn and is, therefore, transferred to the sample. Other parameters that can be controlled are the displacement, travel speed of the horn, trigger force, and hold force. Previous studies have shown how the processing parameters can impact the resulting weld in terms of strength, thickness, and processing temperature [10]. Studies have also established relationships between the processing parameters such as the weld time, energy delivered, power, and amplitude. For example, increase in the amplitude increases the energy delivery and the weld strength, with exception of extremely low amplitudes [11].

Because welding multiple plies of continuous carbon fiber-reinforced thermoplastic composite prepreg is different from joining two thermoplastic parts, it is important to study the welding mechanism and the stage in the welding process. The objective of this study is to apply and optimize the ultrasonic welding process of multiple carbon fiber-reinforced thermoplastic composite plies. Both the temperature development and the distribution were observed at the thickness plane during the welding process using an infrared thermal camera. This study focuses on varying the amplitude and observing the effects on the transient thermal behavior and temperature distribution.

Methodology

The carbon fiber-reinforced thermoplastic composite plies used for this study is APC (PEKK-FC)/AS4D 12K, a unidirectional carbon fiber-reinforced polyether ketone ketone (PEKK) thermoplastic composite prepreg. The glass transition temperature and melting temperature of the PEKK polymer are 159 ºC and 337 ºC, respectively [12]. An ultrasonic welder Sonics H540E with stepped cylindrical titanium horn was used for this study. This welder produces mechanical vibration at 40 kHz frequency and does not have a booster. The convertor outputs an amplitude of 10 µm and the stepped cylindrical horn has a gain of 7.5, resulting in the final amplitude of 75 µm. The amplitude can be controlled from 20 % to 100 % of its maximum amplitude, or from 15 µm to 75 µm in this case. The welding duration can be controlled by either time or energy delivered. Because this ultrasonic welder is a handheld model, a fixture was created to constrict the movement of the welder for controlled welds. A linear ball bearing allows vertical motion for the welder while the pneumatic piston at the top applies a controlled force onto the welder. A flat aluminum anvil was used as it is a common material and only flat samples were welded. A polylactic acid (PLA) sample fixture was 3D-printed to hold a lay-up of the PEKK prepregs. A picture of the fixture and the ultrasonic welder can be seen in Figure 5.

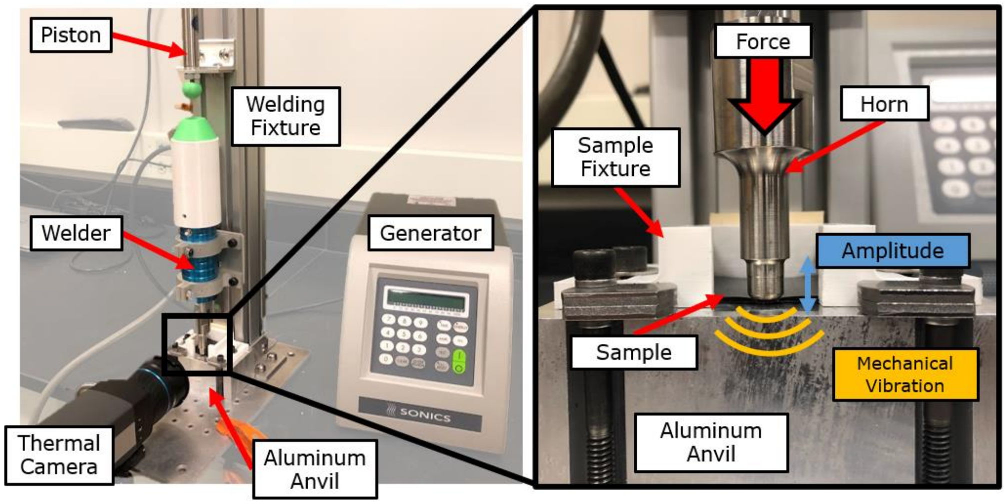

Figure 5. Ultrasonic welding experimental set-up with the thermal camera capturing the thickness plane.

An infrared thermal camera (FLIR A655sc) with an additional 82 mm close-up lens was used to record thermal data throughout the ultrasonic welding process. The carbon fiber-reinforced PEKK material was approximated as a black plastic with an emissivity of 0.94 [13]. To observe the thermal distribution at the cross-section of the weld, the location of horn was placed at the edge of the sample. While this does not provide accurate temperature data for the corresponding welding parameters, it is trivial for the objective of observing the relative thermal patterns and behaviors. The thermal camera is placed normal to the cross-sectional surface approximately 100 mm from the sample, as seen in Figure 3.

The welding force was kept constant at 178 N. After preliminary experiments, it was determined that less welding force would yield inconsistent welds from the variation in ply-to-ply interface contact conditions. The amplitude was varied from 15.0 to 75.0 µm in increments of 7.5 µm. The welding duration was undetermined, but the welding was stopped when the maximum temperature reached steady state. In other words, the process was observed until the welding was complete and there were no new thermal behaviors to be observed.

The sample lay-up was 8 plies of alternating 0º and 90º fiber orientations. The sample dimension was 38.1 x 38.1 mm, and all 4 edges of the sample were used for testing. The sample was installed into the holder, the welding horn was placed on top of the sample, and then the welding force was applied by the pneumatic piston. The thermal camera recorded at around 50 Hz and soon after the ultrasonic welding started according to the different amplitude parameters. Once the maximum temperature was at steady-state, or all the significant welding thermal behavior was observed, the welding was stopped. Multiple trials were conducted for each amplitude to depict accurate transient thermal behavior and patterns.

Results and Discussion

The 15.0 to 37.5 µm amplitude welding processes all resulted in incomplete welding where none of the plies welded together. The heat generation from the mechanical vibration was initially greater than the heat loss to the surroundings but gradually became equal as the temperature rose. Ultimately, the temperature reached steady-state below the necessary temperature for welding. Figure 6 shows these transient maximum temperature responses. The plateau temperatures of the incomplete welds were 29, 39, 50, and 72 °C for 15.0, 22.5, 30.0, and 37.5 µm amplitudes, respectively. All the plateau maximum temperatures were lower than 159 °C, which is the glass transition temperature for the PEKK. It is important to note that Figure 6 and nearly all following thermal data uses the maximum temperature data in each frame, because the average temperature of the welding region is highly dependent on the defined region of interest.

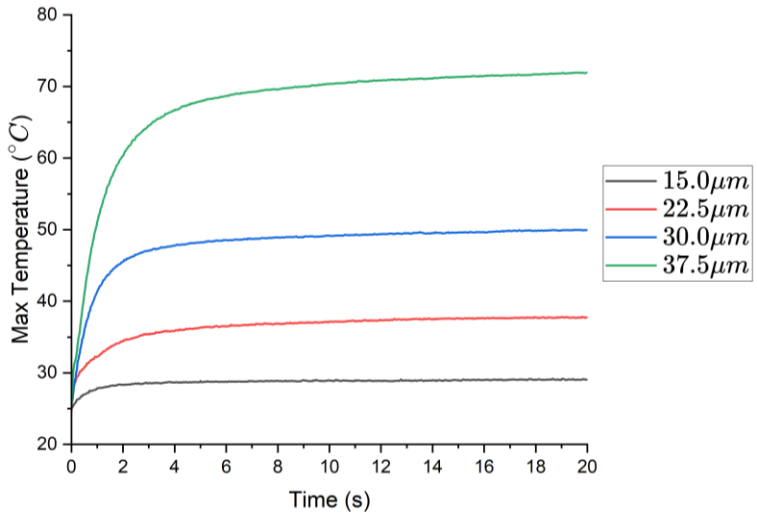

Figure 6. Transient maximum temperature responses of incomplete ultrasonic welds (15.0 to 37.5 µm amplitudes).

Amplitudes of 45.0 µm or greater successfully welded all 8 plies together. The thermal data showed the different stages of welding that were best observed in the 45.0 µm amplitude welding temperature response as shown in Figure 7. The first region, referred to as the build-up stage (a), gave a similar transient temperature response as the incomplete welds, where the plies rise in temperature individually as shown in Figure 8 (a). The rise in temperature gradually decreased as the temperature rose. Instead of settling at a steady-state temperature, the temperature reached a point where the polymer started to soften. This second stage, referred to as the welding stage (b), can be visually observed by the downward displacement of the horn. At this stage, the material softened enough for the contact resistance between the plies to decrease, which caused the mechanical vibrations of ultrasonic welding to transfer more effectively. Figure 8 (b) shows how the weld temperature during this stage rises as a single body. The heat generation, and consequently the rise in temperature, happened faster. While it could not be recorded due to current instrumentation limitations, the instantaneous power delivered that was measured by the generator was also observed to significantly increase at this stage. To further analyze the correlation between the material properties and the welding thermal behavior, the average weld temperature was calculated with the region of interest being only the cross-sectional area under the contact region of the horn and the sample. As the average temperature approaches the glass transition temperature, the rise in temperature slows and settles. At this final stage, referred to as the steady-state stage (c), the material has softened enough that the mechanical vibrations were not effectively transferred and turned into heat within the sample.

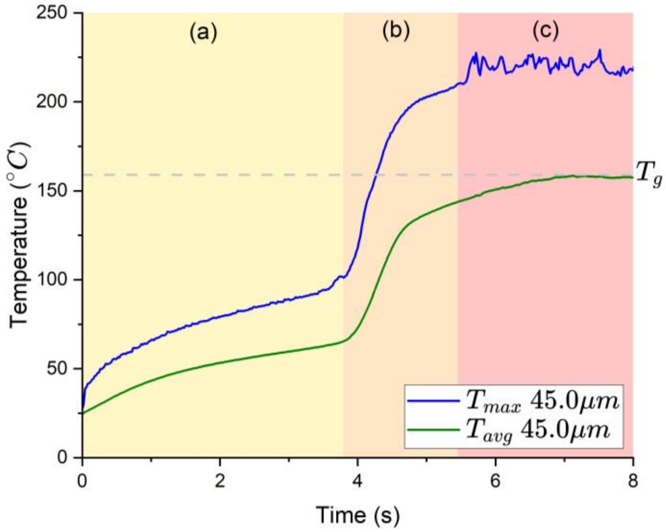

Figure 7. Transient maximum temperature response of 45.0 µm amplitude ultrasonic welding process and T_g of PEKK (159 °C). (a) build-up stage, (b) welding stage, (c) steady-state stage.

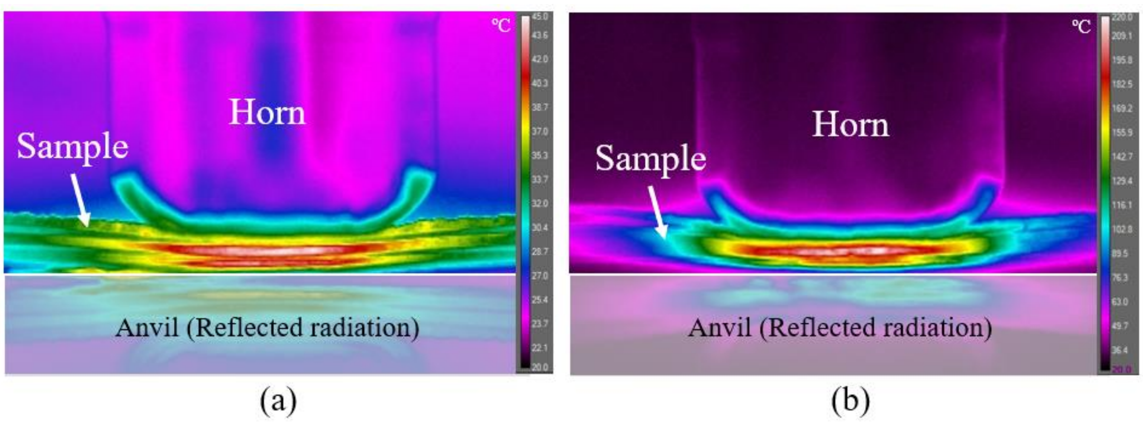

Figure 8. (a) Built-up stage showing plies rising in temperature individually. (b) Welding stage showing horn displacement and temperature rising as single body.

Figure 9 shows transient temperature responses of amplitudes 52.5 to 67.5 µm. The main difference compared to the 45.0 µm amplitude response was that it became harder to identify the transition between the build-up stage and the welding stage, because the temperature rose at similar rates during both stages. However, there were often brief drops in temperature at this transition, potentially due the decreased welding force for a short period of time as the material softens quickly. The other main difference was the overshoot in transient temperature responses, which were due to the faster energy deliveries and temperature rise rates. With greater amplitude, the rate of temperature increase and the peak temperature was greater, leading to overshoot in processing temperature before reaching a lower steady-state temperature. It was also visually observed that higher amplitudes resulted is greater displacement of the horn and consequently more local fiber distortion around the weld.

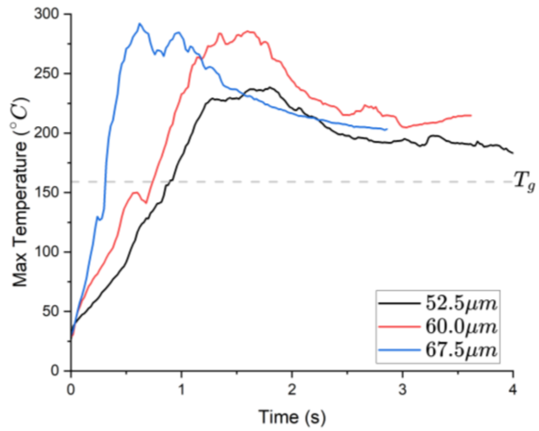

Figure 9. Transient maximum temperature responses of 52.5 to 67.5 µm amplitude ultrasonic welding processes. The T_g and T_m of PEKK are 159 °C and 337 °C, respectively.

Lastly, Figure 10 shows a typical 75.0 µm amplitude transient maximum temperature response. The overshoot was present, and the transition between the build-up and welding stage was unidentifiable by the temperature response. Unlike the 67.5 µm amplitude and below, the maximum temperature went significantly above the melting temperature, which indicated potential thermal degradation to the polymer. The steady-state temperature was also higher at around 280 °C, and prolonged time at this temperature caused significant fiber distortion as the constant welding force deformed the softened layup. With the material being squeezed out due to the low viscosity at the melting temperature, the recorded temperature response often had a lot of noise or multiple spikes resulting from the flow of the molten polymer. With inappropriate welding parameter such as the 75.0 µm amplitude, the damage was not only in the polymer, but the fibers as well. Figure 11 shows a comparison between a weld with an appropriate welding processing parameter and a weld with an inappropriate welding processing parameter. There was significant distortion and wrinkles in the fibers, and the depth of the weld was significantly deeper. In other words, the resulting weld was significantly thinner.

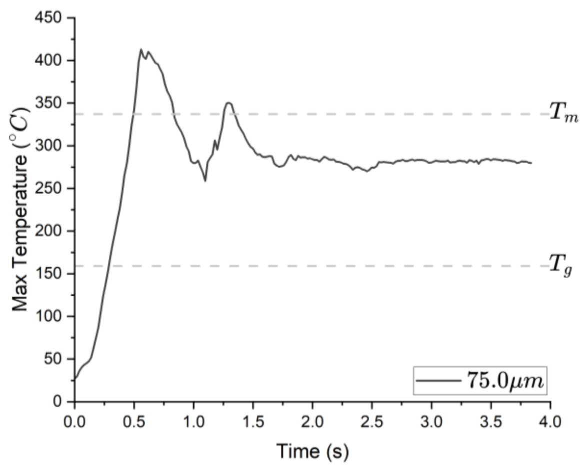

Figure 10. Transient maximum temperature responses of 75.0 µm amplitude ultrasonic welds. The T_g and T_m of PEKK are 159 °C and 337 °C, respectively.

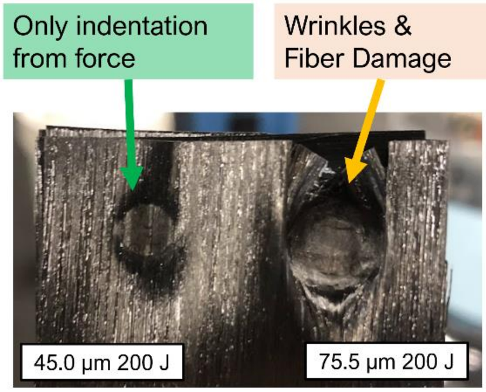

Figure 11. Comparison between ultrasonic weld with appropriate parameter (left) and inappropriate parameter (right).

Conclusion

In this study, the thermal behavior of ultrasonic welding multiple continuous carbon fiber-reinforced thermoplastic composite plies revealed the different stages of welding by testing various amplitudes. The lower amplitude cut-off was identified where the temperature was not sufficient to soften and weld the plies together. The three stages, referred to as the build-up, welding, and steady-state stage, were identified for successful welding processes. During the build-up stage, the plies rose in temperature individually. As the material started to soften, the plies no longer heated up individually, but rose in temperature faster as a single body. Then the temperature settled at a steady-state temperature. Overshoot in maximum temperature responses were also present for higher amplitudes. Higher amplitudes generally resulted in faster increases in temperature, higher peak temperatures, and higher steady-state temperatures. Inappropriate or extremely high amplitudes showed potential for polymer and fiber damage, such as fiber distortion or breakage, and thermal degradation. Therefore, it can be concluded that for the ultrasonic welding of multiple fiber-reinforced thermoplastic composite plies, there is an optimal range of ultrasonic welding parameter to create successful welds without fiber or polymer damage to a final thermoformed part.

Acknowledgements

I would like to thank Purdue University and the Composite Manufacturing and Simulation Center for supporting and advising my research about ultrasonic spot-welding continuous carbon-fiber reinforced thermoplastic composite plies.

Bibliography

[1] Vaidya UK, Chawla KK. Processing of fibre reinforced thermoplastic composites. International Materials Reviews. 2008. p. 185–218.
[2] Barile M, Lecce L, Iannone M, et al. Thermoplastic Composites for Aerospace Applications. Revolutionizing Aircraft Materials and Processes. Cham: Springer International Publishing; 2020. p. 87–114.
[3] Offringa AR. Thermoplastic composites-rapid processing applications. Composites: Purr A. 1996.
[4] Scherer R, Friedrich K. Inter-and intraply-slip flow processes during thermoforming of CF /w-laminates.
[5] Friedrich K, Hou M, Krebs J. Thermoforming of Continuous Fibre-Thermoplastic Composite Sheets.
[6] Okine RK. Analysis of Forming Parts from Advanced Thermoplastic Composite Sheet Materials*.
[7] Slange TK, Warnet L, Grouve WJB, et al. Influence of preconsolidation on consolidation quality after stamp forming of C/PEEK composites. AIP Conf Proc. American Institute of Physics Inc.; 2016.

[8] Bhudolia SK, Gohel G, Leong KF, et al. Advances in ultrasonicwelding of thermoplastic composites: A review. Materials. 2020;13.
[9] Benatar A, Eswaran R V., Nayar SK. Ultrasonic welding of thermoplastics in the near-field. Polym Eng Sci. 1989;29:1689–1698.
[10] Tolunay MN, Dawson PR, Wang KK. Heating and bonding mechanisms in ultrasonic welding of thermoplastics. Polym Eng Sci. 1983;23:726–733.
[11] Villegas IF. In situ monitoring of ultrasonic welding of thermoplastic composites through power and displacement data. Journal of Thermoplastic Composite Materials. 2015;28:66–85.
[12] Solvay. APC (PEKK-FC) Thermoplastic polymer prepreg [Internet]. Alpharetta; 2017 [cited 2023 Jun 25]. Available from: www.solvay.com.
[13] Chen H-Y, Chen C. Determining the emissivity and temperature of building materials by infrared thermometer. Constr Build Mater. 2016;126:130–137.